Supplementary Document: Si-Based Earth Abundant Clathrates for Solar Energy Conversion

Yuping He,[1] Fan Sui,[1] Susan M. Kauzlarich,[1] and Giulia Galli[2,*]

[1] *Department of Chemistry, University of California, Davis, CA 95616*

[2] *The Institute for Molecular Engineering, The University of Chicago, IL 60637*

*Electronic address: gagalli@uchicago.edu

I. SYNTHESIS

Potassium (Acros Organics 98%), Aluminium metal shot (99.99 %) and Silicon lump (Alfa Aesar, 99.9999+%) were cut and weighed in an Argon-filled glove box with the ratio of 9:9:38. These reagents were then transferred into a niobium ampoule which was sealed under argone atmosphere by an arc-welder. The niobium ampoule was then sealed in a fused silica tube under vacuum and annealed at 950^{o}C for 10h and 700^{o}C for 40 h in an electric box furnace. After annealing, the niobium tube was opened in a glove box and excess potassium and aluminium were removed by washing the sample with ethanol and diluted hydrochloric acid as the clathrate phase is stable towards both of them. The product consisted of crystals and dark grey powder.

II. SINGLE-CRYSTAL X-RAY DIFFRACTION

A crystal of $K_8Al_8Si_{38}$ was mounted in MiTeGen micro loop and data were collected at 90 K by Bruker SMART APEXII diffractometer with graphite-monochromatized Mo Kα radiation (λ=0.71069 $\AA$). Analytical absorption correction was performed using SADABS. The stucture solution was obtained by direct methods and refined by full-matrix least squares refinement against F_0^2 using the SHELXTL package. (See Table SI)

III. OPTICAL ABSORPTION SPECTROSCOPY

Polycrystalline sample $K_8Al_8Si_{38}$ was dispersed in ethanol by sonication. The dispersed sample was then spin coated onto a glass slide. The optical absorption spectrum of the sample was measured using a PerkinElmer Model Lambda 750 UV/Vis/NIR spectrophotometer in the range of 400$\sim$1500 nm. The low energy background induced by the scattering in the measurement was not substracted from the absorption spectrum of Fig.3 of the manuscript. Therefore the baseline of spectrum is not at zero, and the Tauc plots with different exponents (square and square root) exhibit differences in their baselines(See Fig.S5 and S6).

IV. HALL COEFFICIENT MEASUREMENT

Polycrystalline sample $K_8Al_8Si_{38}$ was sintered into a bar with the diameter of 4mm at 908 K by a spark plasma sintering system (SPSS). The sintered sample was further cut and polished into a 2.18 x 3.14 x 5.62 mm cuboid for Hall coefficient measurement. Within a Quantum Design Physical Property Measurement System (PPMS), a five-wire measurement was employed to measure the Hall Coefficient, and a four-wire measurement was performed on the sample to determine its electrical resistivity at 300 K. The Hall coefficient value at 7 Tesla was found to be -4.7871 cm^3/coul (see Fig. S7), yielding an electron carrier concentration (n) of 1.3x10^{18} cm^{-3}. The measured electrial resistivity (ρ) is 0.1227 Ωcm. Using $\rho^{-1} = ne\mu$, we obtained an electron mobility (μ) of 39 cm^2/V/s.

V. AB INITIO CALCULATIONS

The configurations of all Si-based type I clathrates were generated starting from the geometry of Si_{46} [1], where K atoms were inserted into the eight cages to obtain a model of K_8Si_{46}; we then randomly substituted eight Si with Al atoms over the three host sites: 6c, 16i and 24k to obtain $K_8Al_8Si_{38}$ with an ideal stoichiometric ratio. We generated six configurations, whose geometry was optimized with respect to the volume and atomic positions using Density Functional Theory (DFT) calculations with the PBE functional [2, 3] and the quantum espresso code [4]. We employed plane wave basis sets and norm conserving pseudopotentials [5].

---

[1] G. B. Adams, M. O'Keeffe, A. A. Demkov, O. F. Sankey, and Y.-M. Huang, Phys. Rev. B **49**, 8048 (1994).

[2] J. P. Perdew, K. Burke, and M. Ernzerhof, Phys. Rev. Lett. **77**, 3865 (1996).

[3] J. P. Perdew, K. Burke, and M. Ernzerhof, Phys. Rev. Lett. **78**, 1396 (1997).

[4] P. Giannozzi et al., http://www.quantum-espresso.org.

[5] D. R. Hamann, M. Schlüter, and C. Chiang, Phys. Rev. Lett. **43**, 1494 (1979).

TABLE SI: Crystallography data and structure refinement parameters for the clathrate with nominal composition $K_8Al_8Si_{38}$ synthesized in this work.

Chemical Formula [a]	$K_8Al_{7.63}Si_{38.37}$
Space Group	Pm$\bar{3}$n (No. 223)
Lattice Constant ($\mathring{A}$)	10.4802(16)
Volume ($\mathring{A}^3$)	1151.1(3)
Density (Calc. g/cm^3)	2.301
Z	1
Absorption coeff(mm^{-1})	1.905
θ	2.75-27.5
Reflns Collected	15227
Independent Reflns	264 [R(int)=0.03]
Data/restraints/params	264/0/17
GOF on F^2	0.860
Final R indices[$I > 2\sigma(I)$] [b]	R_1=0.0113; wR_2=0.0322
R indices (all data)	R_1=0.0122; wR_2=0.0313
Largest diff. peak and hole eÅ^{-3}	0.24 and -0.15

[a]Determined from X-ray Crystallography

[b]$R_1 = \frac{\sum ||F_0|-|F_c||}{\sum |F_0|}$; $wR_2 = (\sum(F_0^2 - F_c^2)^2)^{1/2}$; $w^{-1} = \sigma^2(F_0) + (0.0220P)^2 + 1.04P$, where $P = max(F_0^2, 0) + 2F_c^{2/3}$

TABLE SII: Atomic coordinates and equivalent isotropic displacement parameters (U_{eq}) for $K_8Al_8Si_{38}$.

Label	Wyckoff site	x	y	z	Occupancy	$U_{eq}(\mathring{A}^2)$ [a]
K1	2a	0.0000	0.0000	0.0000	1.0000	0.0059(2)
K2	6d	0.2500	0.5000	0.0000	1.0000	0.01224(16)
Si1	24k	0.0000	0.30346(3)	0.11688(4)	0.879(19)	0.00563(15)
Al1	24k	0.0000	0.30346(3)	0.11688(4)	0.121(19)	0.00563(15)
Si2	16i	0.18430(2)	0.18430(2)	0.18430(2)	1.0000	0.00577(14)
Si3	6c	0.0000	0.5000	0.2500	0.21(8)	0.0056(4)
Al3	6c	0.0000	0.5000	0.2500	0.79(8)	0.0056(4)

[a]U_{eq} is defined as one-third of the trace of the orthogonalized U_{ij} tensor.

TABLE SIII: Atomic distances between Wyckoff sites in two models of $K_8Al_8Si_{38}$: the $5c2k1i$ model (Al occupies: five $6c$, two $24k$ and one $16i$ sites) and the $6c2i$ model (Al occupies: six $6c$ and two $16i$ sites), compared with the experimental values obtained from single crystal XRD measurement.

Atomic site	$5c2k1i$	$6c2i$	Exp.
$24k - 6d$	3.57,4.06	3.62,4.11	3.5509,4.0540
$16i - 6d$	3.93	3.93	3.8925
$6c - 6d$	3.83	3.74	3.7053
$24k - 2a$	3.48	3.42	3.40792
$16i - 2a$	3.37	3.36	3.3456
$24k - 24k$	2.46	2.44	2.4501
$6c - 24k$	2.44		2.4879
$16i - 24k$	2.43	2.43	2.4061
$16i - 16i$	2.42	2.43	2.3848

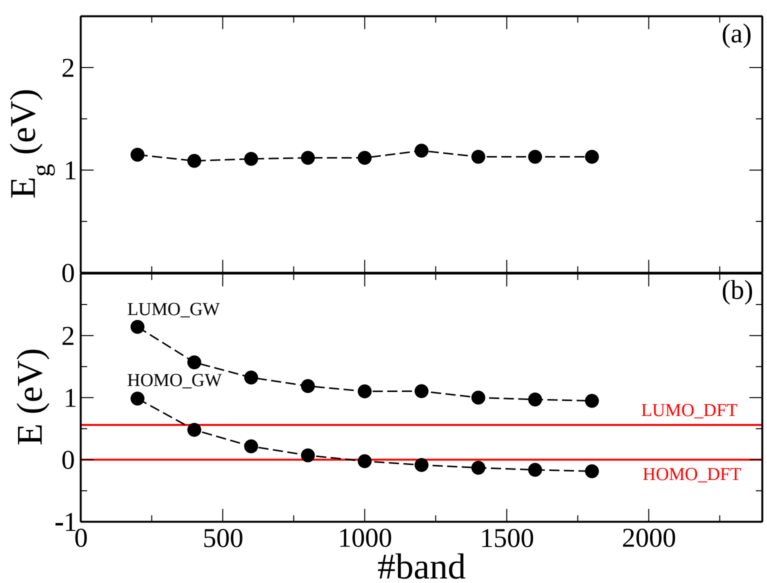

FIG. S1: (a)Computed G_0W_0 direct band gap at Γ, as a function of the number of bands included in the calculation for the $K_8Al_8Si_{38}$ sample A (5c2k1i). (b)Computed G_0W_0 single particle energies of HOMO and LUMO states as a function of the number of bands included in the calculation for sample A; the corresponding values obtained using DFT and the PBE functionals are indicated by the red lines.

TABLE SIV: Total energy differences (ΔE) of samples A,B,C,D and E ($K_8Al_8Si_{37}$) with respect to that of sample B (see Table I) computed by DFT-PBE. As shown in column two (black spheres represent the missing Si atom), in samples A, B and C a Si atom was removed from the 6c site; the resulting vacancy had only one Al neighbor in A and B (on the 16i and 6c site, respectively), but two Al neighbors in C (one on 6c and the other one on 16i); in samples D and E a Si atom was removed from 16i and 24k, respectively and the resulting vacancy had no Al neighbors.

Sample	Vacancy	ΔE (eV)	Electronic Properties
A	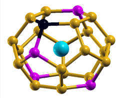	0.19	metal
B	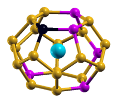	0.00	semicondutor
C	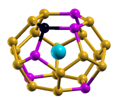	0.00	semiconductor
D	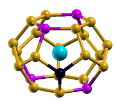	1.04	metal
E	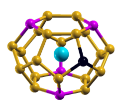	1.08	metal

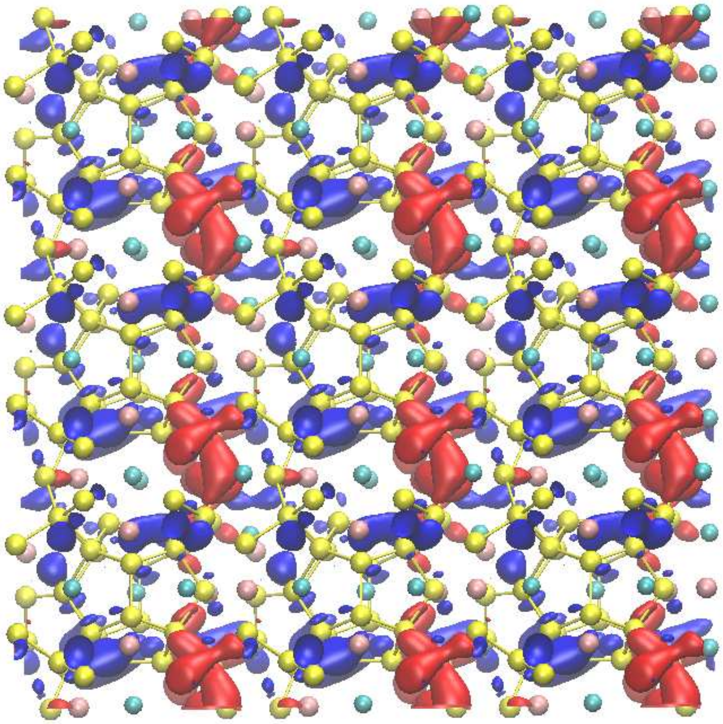

FIG. S2: Isosurfaces of the square moduli of the valence band maximum (red) and conduction band minimum (blue) single particle states of type I clathrate $K_8Al_8Si_{38}$ (sample B); yellow, pink and cyan spheres represent Si, Al and K atoms, respectively.

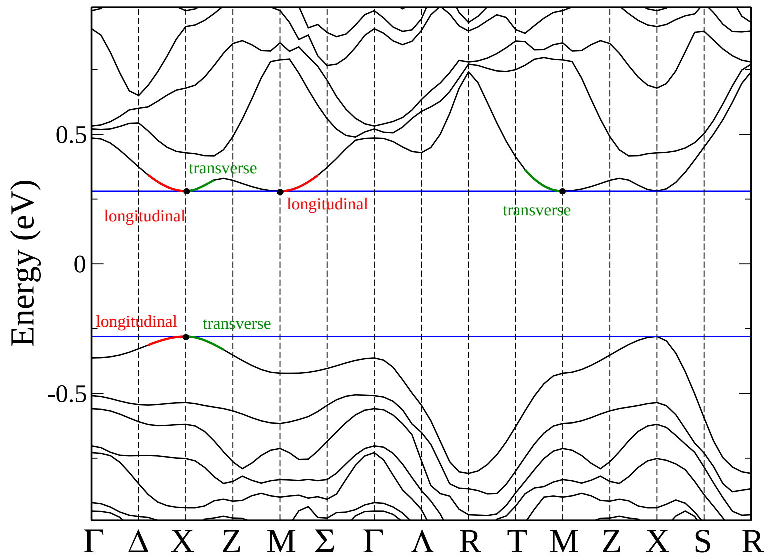

FIG. S3: Band structure of $K_8Al_8Si_{38}$ (sample A) calculated using DFT-PBE. Red curves and green curves represent the quadratic fits of bands used for the longitudinal effective mass ($m^*_{||}$) and transverse effective mass $m^*_{\perp}$ calculations.

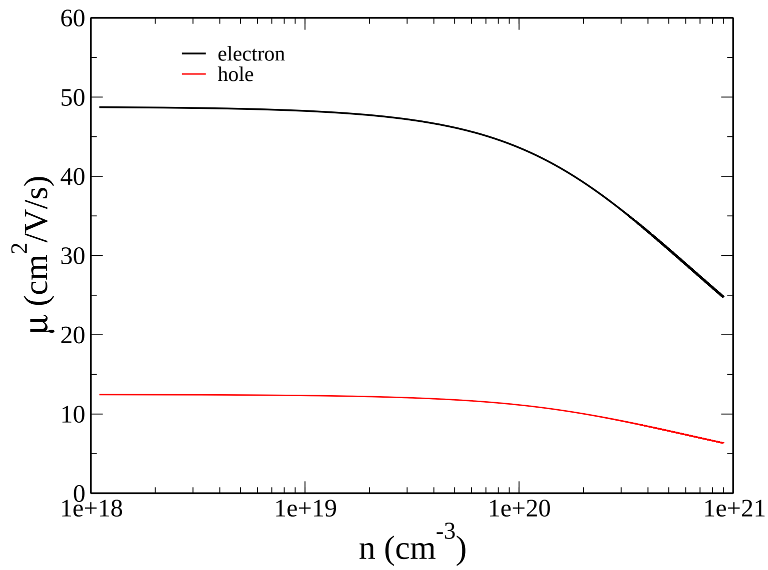

FIG. S4: Calculated electron (black line) and hole (red line) mobilities of type I clathrate $K_8Al_8Si_{38}$ as a function of carrier concentration (n) at room temperature, using the single Kane band model.

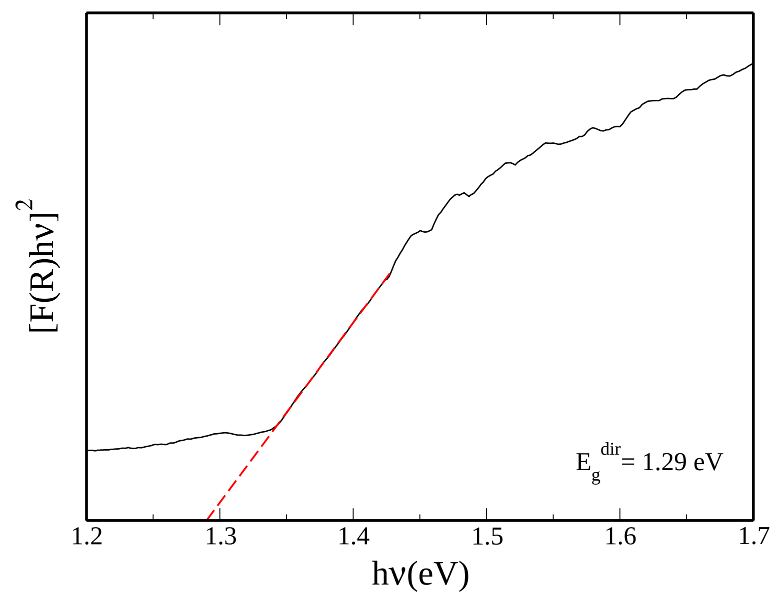

FIG. S5: The function $[F(R)h\nu]^2$, where $F(R)=(1-R^2)/2R$ and R is the measured reflectance, as a function of the photon energy hν. The dotted line is a fit to: $[F(R)h\nu]^2 = A^{dir}(h\nu - E_g^{dir})$

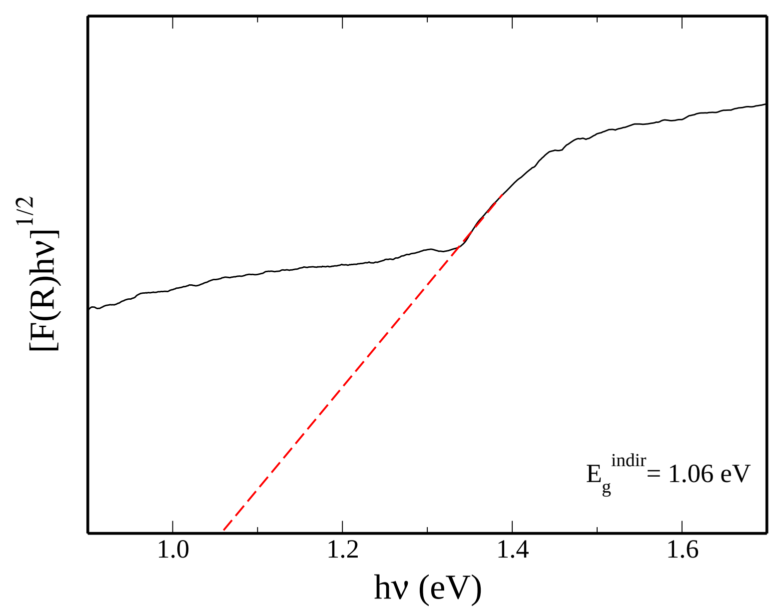

FIG. S6: The function $[F(R)h\nu]^{1/2}$, where $F(R)=(1-R^2)/2R$ and R is the measured reflectance, as a function of the photon energy h$\neq$. The dotted line is a fit to: $[F(R)h\nu]^{1/2} = A^{indir}(h\nu - E_g^{indir})$

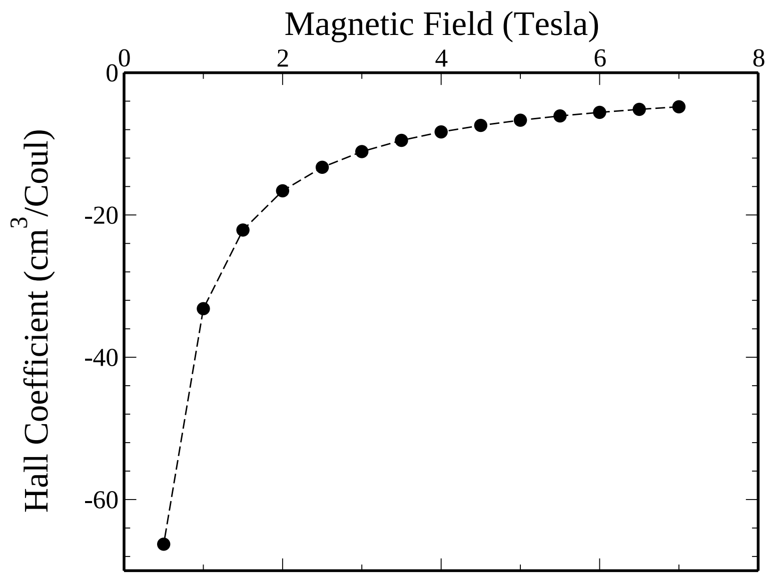

FIG. S7: Hall coefficient as a function of magnetic field